

DEVELOPMENT AND APPLICATION OF A TIME-HISTORY ANALYSIS  
FOR ROTORCRAFT DYNAMICS BASED ON A  
COMPONENT APPROACH

Robert Sopher  
Supervisor, Dynamics Methods

Daniel W. Hallock  
Dynamics Engineer

Sikorsky Aircraft Division  
United Technologies Corporation, Stratford, CT

Abstract

This paper describes a time-history analysis for rotorcraft dynamics based on dynamical substructures, and non-structural mathematical and aerodynamic components. The analysis is applied to predict helicopter ground resonance and response to rotor damage. Other applications illustrate the stability and steady vibratory responses of stopped and gimbaled rotors, representative of new technology. Desirable attributes expected from modern codes are realized, although the analysis does not employ a complete set of techniques identified for advanced software. The analysis is able to handle a comprehensive set of steady state and stability problems with a small library of components. It has responded to new technologies with timely solutions by limiting the effort required to implement new capabilities through its component structure. Opportunities were taken to reduce development costs by addressing more than one type of problem with a single component, such as using a minimum variance controller for trim and vibration reduction.

Notation

B = matrix, Eq. (20),  $N \times N$   
 C = independent coordinate system damping matrix,  $N \times N$   
 $C_D$  = dependent coordinate system damping matrix,  $N_D \times N_D$   
 $C_t$  = rotor thrust coefficient  
 D = matrix, Eq. (15),  $N \times N$

Paper presented at "Second Decennial Specialists' Meeting on Rotorcraft Dynamics", American Helicopter Society, NASA Ames Research Center, Moffett Field, California, November 7-9, 1984.

$[c]^{(i)}$  = damping matrix for i-th substructure  
 $\{f\}^{(i)}$  = vector of external forces for i-th sub-structure, representing forces and moments.  
 $f_{x1} \ f_{y1} \ f_{z1}$  = components of force applied to a substructure connection node, Fig. 2, 1b  
 h = time interval in Newmark-Beta method, Eq. (10), sec.  
 F = independent coordinate system force vector,  $N \times 1$   
 $F_D$  = dependent coordinate system force vector,  $N_D \times 1$   
 $F'$  = matrix, Eq. (21),  $N \times N$   
 I = unit matrix,  $N \times N$   
 K = independent coordinate system stiffness matrix,  $N \times N$   
 $K_D$  = dependent coordinate system stiffness matrix,  $N_D \times N_D$   
 $[k]^{(i)}$  = stiffness matrix for i-th substructure  
 M = independent coordinate system mass matrix,  $N \times N$   
 $M_D$  = dependent coordinate system mass matrix,  $N_D \times N_D$   
 $[m]^{(i)}$  = mass matrix for the i-th substructure

$m_{x1}$   $m_{y1}$   $m_{z1}$  = components of moment applied to a substructure connection node, Fig. 2, lb-ft  
 $n$  = integer step number in time-history solution, Eq. (10)  
 $N$  = total number of independent coordinates in the assembled system.  
 $N_D$  = total number of coordinates in the dependent coordinate vector (obtained by summing the coordinates for all substructures)  
 $P$  = matrix, Eq. (16),  $N \times N$   
 $Q$  = matrix, Eq. (17),  $N \times N$   
 $\{r\}^{(i)}$  = vector of reaction loads applied to the  $i$ -th substructure  
 $r_{x1}$   $r_{y1}$   $r_{z1}$  = components of reaction force applied to a substructure connection node, Fig. 2, lb  
 $r_{mx1}$   $r_{my1}$   $r_{mz1}$  = components of reaction moment applied to a substructure connection node, Fig. 2, lb-ft  
 $R$  = matrix Eq. (19),  $N \times N$   
 $R_D$  = dependent coordinate system reaction load vector,  $N_D \times 1$   
 $t$  = time, sec  
 $u$   $v$   $w$  = displacements at a connection node, ft  
 $\{x\}^{(i)}$  = vector of coordinates for  $i$ -th substructure  
 $x_1$   $y_1$   $z_1$  = rectangular coordinates, Fig. 2  
 $X_D$  = vector of dependent coordinates for the system,  $N_D \times 1$ , Eq. (3)  
 $X_I$  = vector of independent coordinates for the system,  $N \times 1$   
 $\beta$  = transformation matrix relating dependent coordinates to independent coordinates Eq. (4),  $N_D \times N$

$\beta^*$  = Newmark-Beta factor  
 $\beta_0, \beta_1, \beta_2$  = transformation matrices from which  $\beta$  is constructed, Eq. (9)  
 $\theta_1$   $\theta_2$   $\theta_3$  = angular displacements at a connection node, Fig. 2, rad.  
 $\sigma$  = rotor solidity  
 $\mu$  = rotor advance ratio, non-dimensional  
 $\psi$  = rotor azimuth angle, rad  
 $\Omega$  = rotor speed, rad/s  
 $[0]$  = matrix of zeroes

#### Subscripts

$n$  = time index  
 $D$  = dependent coordinate system variable

#### Superscripts

$i$  =  $i$ -th substructure  
 $T$  = transpose  
 $\cdot$  = first derivative with respect to time  
 $\ddot{\phantom{x}}$  = second derivative with respect to time

#### Introduction

In the 1970's dissatisfaction with first generation computer programs for predicting helicopter performance and dynamic behavior motivated the development of the Second Generation Comprehensive Helicopter Analysis System (2GCHAS). The project is funded by the U.S. Government and is managed by the 2GCHAS Project Office at the NASA/Ames Research Center, and involves the participation of industry. The 2GCHAS system aims to provide results for several helicopter related engineering disciplines, as well as helicopter dynamics.

Several approaches were identified as being of potential value for overcoming first generation deficiencies. These approaches consisted of the use of a unifying mathematical basis, executive-based software, and software design and management methodology.

One promising mathematical approach is to separate the dynamical structure into several components, or substructures, and subsequently to combine these into a system of second order differential equations. Coupled with automated assembly of the components, substructuring is expected to enable many problems to be modeled, overcoming the lack of versatility characteristic of first generation systems. Substructuring should reduce the difficulties of verifying the code by dividing the system into easily verifiable parts. Activity can be focused on areas of new code during the process of adding new components, making the system more responsive to changes.

In parallel with this, a software executive would be used to enhance system versatility and usage for components which could not be handled as dynamical substructures, such as post-processing modules and certain types of aerodynamic components.

Application of the techniques of structured design, developed in the software industry (Ref. 1), would help to improve architecture, and coding standards would make code legible. As a result, a second generation system would become more productive by being able to lead a longer useful life and would become more credible because it could be more easily verified. Finally, software management methodology, including automated software tools, would be used for configuration control of versions of the system by protecting versions from untested and undocumented changes.

The cost of applying all the approaches mentioned above to create a system with the scope of 2GCHAS appears to be beyond the resources of any single helicopter manufacturer. On the other hand, recognizing that benefits might result from application of a part of these approaches, the U.S. industry developed experimental codes utilizing some of the new concepts and limited to solution of dynamic problems (Refs. 2 to 4). Sikorsky has developed two component-based codes consisting of the Simplified Vibration Analysis (SIMVIB) of Ref. 2, and the Rotorcraft System Dynamics Analysis (RDYNE) described in this paper. Both methods utilize the same code for substructure assembly, but component libraries are different, providing solutions which differ in technique and scope. In contrast to SIMVIB which emphasizes harmonic balance solutions, RDYNE is a time-history analysis. It is the purpose of the paper to describe RDYNE, particularly with a view to its second generation attributes.

### Basis of Analysis

The helicopter dynamical system is assumed to be made up of dynamical substructures and these are automatically assembled into a coupled system represented by a second order differential matrix equation. Figure 1 shows a typical substructure breakdown of a helicopter. The method is able to assemble components into many combinations and orientations. Coupled system response is obtained by integrating the differential equation with respect to time.

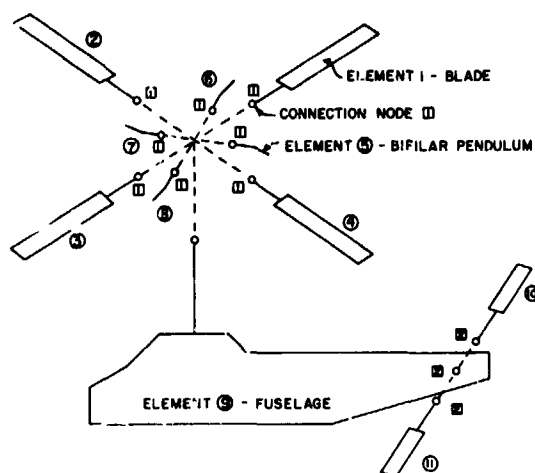


Fig. 1 Sample Substructures Used in the RDYNE Rotorcraft Dynamics Analysis

### Substructure Assembly Method

The substructure method employed is the Hurty method of Ref. 5. The coordinates or degrees of freedom of a substructure (also called physical component) are physical and generalized displacements, such as modal amplitudes. The matrix equation of motion for each substructure is expressed in mass, damping, and stiffness matrix, and force vector form. Properties of the  $i$ -th substructure are  $[m]^{(i)}$ ,  $[c]^{(i)}$ ,  $[k]^{(i)}$ ,  $\{f\}^{(i)}$ , and  $\{r\}^{(i)}$ . These are respectively mass, damping, and stiffness matrices, and external force and reaction force vectors. The submatrices for the substructures are collected into a partitioned diagonal matrix equation which represents the system. This partitioned diagonal matrix equation is

$$M_D \ddot{X}_D + C_D \dot{X}_D + K_D X_D = F_D - R_D \quad (1)$$

The matrix  $M_D$  illustrates the typical form of the diagonal matrices as:

$$M_D = \begin{bmatrix} [m]^{(1)} & & \\ & [m]^{(2)} & \\ & & \ddots \\ & & & [m]^{(i)} \end{bmatrix} \quad (2)$$

The vector of coordinates  $X_D$  illustrates the form of the vectors  $F_D$  and  $R_D$  in Eq. (1), and is

$$X_D = \begin{Bmatrix} \{x\}^{(1)} \\ \{x\}^{(2)} \\ \vdots \\ \{x\}^{(i)} \end{Bmatrix} \quad (3)$$

The coordinate vector  $X_D$  contains unconnected (or internal)  $X_D$  coordinates and connection node coordinates. When components are to be connected to each other, redundant coordinates occur in  $X_D$ . Fig. 2 shows the translational and rotational displacements, and forces and moments on a connection node.

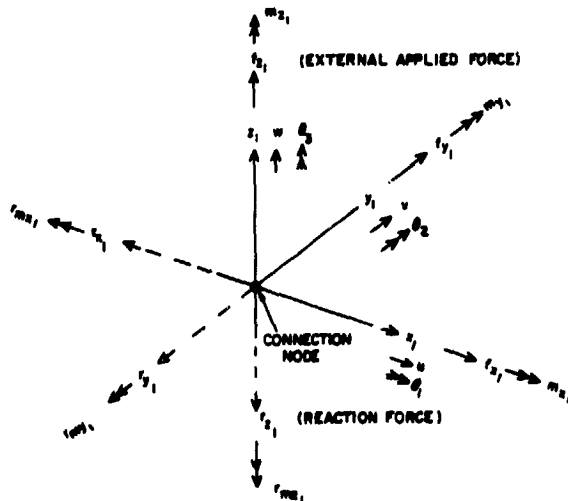


Fig. 2 Displacements and Forces Acting on a Connection Node of a Substructure

The synthesis of the equations of motion for the coupled system is accomplished by a mapping relating the dependent coordinates,  $X_D$ , to a reduced (or independent) coordinate set,  $X_I$ . Redundant coordinates are eliminated by requiring component displacements to be equal at connections. The transformation matrix relating  $X_D$  and  $X_I$  is denoted by  $\beta$ , and the mapping of coordinates is

$$X_D = \beta X_I \quad (4)$$

Substitution of the transformation Eq. (4) in Eq. (1) and premultiplication of equation (1) by  $\beta^T$  yields the final equation of motion for the coupled system. This is

$$M \ddot{X}_I + C \dot{X}_I + K X_I = F \quad (5)$$

The matrices in Eq. (5) are typified by

$$M = \beta^T M_D \beta \quad (6)$$

and the load vector is

$$F = \beta^T F_D \quad (7)$$

The component displacements  $X_D$  may be recovered from the solution to Eq. (5),  $X_I$ , by mapping Eq. (4), and component velocities and accelerations are derived similarly. With  $X_D$  and its derivatives known, connection node or interface reactions (e.g., rotor hub shears) may be determined from Eq. (1).

$$R_D = F_D - (M_D \ddot{X}_D + C_D \dot{X}_D + K_D X_D) \quad (8)$$

The transformation matrix  $\beta$  is the product of three transformations (Ref. 2) which assemble coupled systems from components whose properties are defined in component local axes and allow for the use of modal coordinates. The transformation  $\beta$  is

$$\beta = \beta_0 \beta_1 \beta_2 \quad (9)$$

The transformation from dependent coordinates resolved to local axes with arbitrary angular orientations to dependent coordinates resolved to a global reference axis is  $\beta_0$ . The transformation from dependent coordinates, referred to a global reference axis, to coordinates from which redundant coordinates at connection nodes have been removed is  $\beta_1$ . The transformation from physical domain independent coordinates to coordinates which include modal coordinates,  $X_I$ , is  $\beta_2$ .

#### Time History Solution

The solution algorithm yielding the time history response is the Newmark-Beta method described in Ref. 6. Displacement responses are obtained from displacements known at prior times, and from data defining the magnitudes of known external forces acting on the system.

The vector of coordinates satisfying Eq. (5) at time step  $n$  is denoted  $(X_I)_n$ . The corresponding time is:

$$t_n = t_{n-1} + h \quad (10)$$

In Eq. (10)  $h$  is the step size. The integer step number  $n$  ranges from one to the number of steps in the calculation. Time  $t_0$  is the initial time. Corresponding initial conditions are  $(X_I)_0$  and  $(\dot{X}_I)_0$ .

When  $(X_I)_0$  and  $(\dot{X}_I)_0$  are specified the displacement response at  $t_1$  is found from:

$$(X_I)_1 = D^{-1} [P(X_I)_0 + Q(\dot{X}_I)_0 + \beta^* h^2 F_1 + R F_0] \quad (11)$$

Matrices  $D$ ,  $P$ ,  $Q$  and  $R$  are functions of  $M$ ,  $C$ , and  $K$  in Eq. (5), time step  $h$ , and factor  $\beta^*$  (see equations (15) through (21)). They have dimensions  $N \times N$  where  $N$  is the size of  $X_I$  in Eq. (5). The factor  $\beta^*$  is the Newmark-Beta Factor. Values of  $\beta^*$  ranging from 0 to 0.25 can be input to the program. The factor  $\beta^*$  is used to control the variation of acceleration assumed in the time interval (see remarks in Ref. 6). A numerical solution with  $\beta^* = 0.25$  is unconditionally stable. Force vectors  $F_1$  and  $F_0$  are known external forcing functions at  $t_0$  and  $t_1$ .

After the solution  $(X_I)_1$  is known, successive solutions are obtained from the recursion formula:

$$(X_I)_{n+1} = D^{-1} [B(X_I)_n - F'(X_I)_{n-1} + \beta^* h^2 (F_{n+1} + (1/\beta^* - 2)F_n + F_{n-1})] \quad (12)$$

The  $N \times N$  Matrices  $B$  and  $F'$  are known functions of  $M$ ,  $C$ , and  $K$ , step size  $h$ , and factor  $\beta^*$  (see Eqs. (20) and (21)). Equation (12) may be used to restart solutions from solutions calculated up to the time of restart.

The additional assumption is made in the program code that the force  $F_{n+1}$  linearly extrapolates the forces  $F_n$  and  $F_{n-1}$ . For equal intervals of time  $h$  this assumption reduces to:

$$F_{n+1} = 2F_n - F_{n-1} \quad (13)$$

and Eq. (12) becomes:

$$(X_I)_{n+1} = D^{-1} [B(X_I)_n - F'(X_I)_{n-1} + h^2 F_n] \quad (14)$$

Eq. (13) allows for the insertion of aerodynamic forces which are functions of  $X_I$  and  $\dot{X}_I$ , by assuming  $F$  to be a function of  $X_I$  and its derivatives at a prior time.

Matrices in Eqs. (11), (12), and (14) are:

$$D = M + (h/2)C + \beta^* h^2 K \quad (15)$$

$$P = M + (h/2)C - (1/2 - \beta^*) h^2 K - (1/4 - \beta^*) h^3 C M^{-1} K \quad (16)$$

$$Q = [M - (1/4 - \beta^*) h^2 C M^{-1} C] h \quad (17)$$

$$R = [(1/2 - \beta^*)I + (1/4 - \beta^*) h C M^{-1}] h^2 \quad (18)$$

$$I = \text{unit matrix} \quad (19)$$

$$B = 2M - (1 - 2\beta^*) h^2 K \quad (20)$$

$$F' = M - (h/2)C + \beta^* h^2 K \quad (21)$$

The dimensions of matrices in Eqs. (15) through (21) are  $N \times N$  where  $N$  is the dimension of the vector of independent coordinates  $X_I$ .

#### Main Features of Computer Program

The top-level structure of the computer program reflects the component basis of the analysis. Dynamical components are substructures which obey second order differential equations which can be assembled into coupled dynamical systems. Non-dynamical components include several types of section aerodynamic and inflow models, and a component for trim and vibration reduction.

#### Top-Level Structure of Program

The top level structure of the RDYNE computer program is shown in Fig. 3 and reflects the component basis of the program, showing a separation into component-dedicated and component-independent areas. This organization is responsible for several desirable attributes.

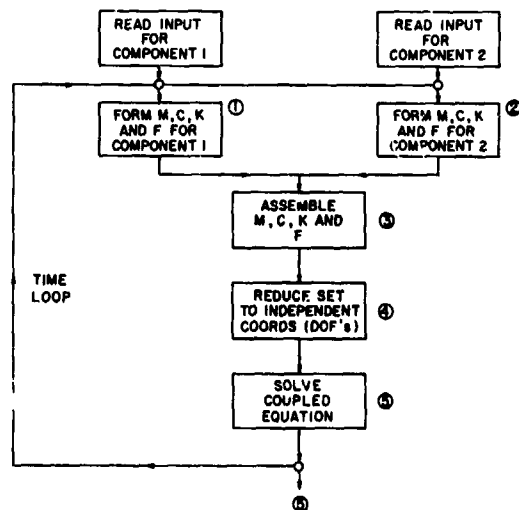


Fig. 3 RDYNE Main-line Program Flow Chart

Component routines are required for each dynamical component listed in Table 1 and a typical organization is shown in Fig. 3. Component input and processing blocks form mass, damping, and stiffness matrices and aerodynamic and gravitational loads at the component level. Component-independent code performs assembly of substructures into a coupled system, reduction to independent coordinates, and solution of the equations. An interpretive routine (not shown in Fig. 3) reads names of selected components and corresponding input, and is followed by processing which utilizes component element numbers and connection node numbers (Fig. 1) and component orientations to assemble components into a coupled system.

Non-dynamical components include several types of section aerodynamic and rotor inflow models, and a component for trim and vibration reduction. The components resemble dynamical components by having dedicated input and processing routines but otherwise do not behave like dynamical substructures because they cannot be assembled into dynamical systems by the assembly method described previously.

Usage and understanding of the program are facilitated by ability of the program to limit input data to components selected by the user for his particular problem. This contrasts with first generation systems which required an understanding of the input for the most comprehensive problem even when preparation of only a part of this input was required. Processing and

storage requirements are limited to the components selected, allowing resources to be tailored to each problem and to be less than the resources for the most comprehensive problem. Verification, modification, and addition of components is confined to component routines, making the system more responsive to change requirements. User and programmer experiences and data on execution speed have confirmed the above attributes.

#### Dynamical Substructures

All dynamical substructures, except modal structures (see text below) employ coordinates which are unconnected (or internal) coordinates, and connection coordinates which enable the substructure to be assembled with other substructures through the equating of displacements at the connection. With the exception of modal structures, it is necessary for each substructure to include six equations of equilibrium corresponding to the six displacements at the connection node shown in Fig. 2, to enable it to be coupled to any other substructure.

A noteworthy difference between dynamical substructures (Table 1) is that the blade models contain matrices which are explicit functions of time while the fuselage and matrix structure in Table 1 have constant matrices. Explicit time dependence occurs from a resolution of blade hub loads to a non-rotating axis system (Fig. 2) to derive the connection node equilibrium equations. This allows the transformation

Table 1 - Dynamical Components in the RDYNE Analysis

<u>Component</u>	<u>Description</u>
Elastic Blade	Normal modes elastic blade with flatwise, edgewise, and torsion elastic modes (Ref. 8), augmented to include six hub displacements, and expressed in M, C, K, and F forms.
Articulated Blade	Simplified model containing a subset of the coordinates applicable to the elastic blade.
Modal Structure	Structure expressed in terms of normal mode coordinates.
Matrix Structure	Generalized structure with fully populated M, C, and K matrices.
Prescribed Force	Substructure providing for the application to any component of a harmonically varying force of specified amplitude and phase.
Fixed Absorber	Vibration absorber which may be attached to any other substructure in the non-rotating system.

matrix  $\beta$  in Eq. (4) to be independent of time, and can be shown to justify the transformation of the dependent coordinate Eq. (1) to the independent coordinate Eq. (5).

The theory of Ref. 8, available in older codes at Sikorsky, was used as the basis of the elastic blade model (Fig. 4) to minimize the labor required to code and check the model, and because this model has been substantiated through extensive comparisons with test data. Although the blade model is available in older codes, completely new coding was written to conform to the component basis and legibility requirements of RDYNE. The equations for the internal coordinates were augmented with six hub equilibrium equations corresponding to hub connection node coordinates. The equations also were reduced to M, C, K, and F forms.

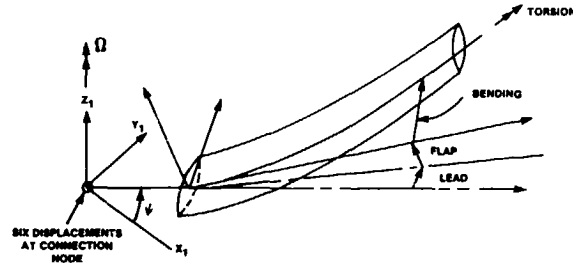


Fig. 4 Schematic of Elastic Blade Substructure

Table 2 - Mathematical and Aerodynamic Components

<u>Component</u>	<u>Description</u>
Time History Integration Method	Component used to integrate the equations of motion with respect to time which employs the Newmark-Beta finite difference method of Ref. 6.
Trim Controller	Minimum variance controller used for rotor trim and coupled system vibration reduction (Ref. 10).
Environment Input	Component defining the properties of the atmosphere.
Aerodynamic Model Type 1	Simplified formula-based section aerodynamic model for conventional airfoils.
Aerodynamic Model Type 2	Table look-up section aerodynamic model for conventional airfoils.
Aerodynamic Model Type 3	Simplified formula-based section aerodynamic model for circulation control airfoils (Ref. 7).
Aerodynamic Model Type 4	Table look-up section aerodynamic model for circulation control airfoils.
Rotor Inflow Type 1	Momentum-based uniform rotor inflow component.
Rotor Inflow Type 2	Variable rotor induced inflow component, using a matrix of wake influence coefficients, calculated by the method described in Ref. 9 and transmitted to RDYNE.
Rotor Inflow Type 3	Momentum-based annulus inflow for hover applications.
Rotor Inflow Type 4	Glauert inflow consisting of steady and first harmonic azimuthal and linear radial variations of inflow.

The modal structure is an exception to the coordinate classification for other substructures. This substructure employs the normal modes of a substructure as coordinates and has constant mass damping, and stiffness matrices, and can be used to represent fuselages, and other systems, described in the applications. Each such structure is allowed to have up to five connection nodes, at which elements of the modal matrix for each normal mode are defined, comprising three translations and three rotations, with the directions shown in Fig. 2. The substructure is coupled to others by expressing physical displacements at a connection as a summation of modes, to define  $\beta_2$ , in Eq. (9).

The aerodynamic generalized forces in the blade components are obtained from application of blade element theory and by invoking the section aerodynamic and inflow components listed in Table 2 to define aerodynamic properties.

#### Aerodynamic Components

Four section aerodynamic and four inflow models are available, and are listed in Table 2. The section aerodynamic models include formula-based and table look-up methods. Input to the formula-based section Aerodynamic Model Type 1 consists of lift curve slope, maximum lift coefficient, and coefficients required in expressions for drag and moment curves. This simple model is used when data on section characteristics are not accurately known, such as in blade damage simulations. Aerodynamic Model Type 2 is used to provide bivariate tables of characteristics expressed as functions of angle-of-attack and Mach number, obtained from wind tunnel tests.

To link an aerodynamic component to a blade component, the user specifies in the input to the blade component the element number of the aerodynamic component, which is followed by corresponding input data or file names defining the location of data. The linkage procedure provides considerable latitude for using different aerodynamic components on different blades and blade sections, and has been well received by users.

Rotor induced variable inflow is embodied in geometric influence coefficients transmitted to a file from an existing program external to RDYNE (Ref. 9). The wake form is a skewed helix and its geometry is assumed to depend on advance ratio. RDYNE determines by an iterative method wake circulations which are consistent with the inflow influencing blade section aerodynamic loads. A strong coupling is

achieved of variable inflow to rotor response in RDYNE without having to rely on a procedure involving iterative coupling of large programs, such as that used for SIMVIB in Ref. 2.

#### Trim and Vibration Reduction

A departure was made with older derivative-based trim determination methodology by treating the trim problem as an optimization problem, and the opportunity was taken to solve both the trim problem and the vibration reduction problem. The code for the controller was derived from the vibration reduction program described in Ref. 10.

A minimum variance controller was implemented which utilized an unconstrained minimization formulation to reduce differences between a target trim state, corresponding to specified steady hub loads, and components of steady hub loads for the actual rotor state. The transfer matrix relating hub loads to control inputs is initially calculated by a difference method from the results of perturbations to the control vector and subsequently is identified by a Kalman filter procedure, which is able to speedily identify the transfer matrix. A scalar performance index embodies the objectives to be minimized and differentiation of the performance index with respect to the control variables yields an optimal control state vector. Controls are updated according to the optimal formula at user-specified intervals.

Figures 5 and 6 show the effects of application of the method to a four-bladed conventional rotor on a rigid support. The simulation employs a single elastic blade and multiplies the steady loads by a factor of four to define the rotor loads. Figures 5 and 6 show that several trim objectives may be specified and simultaneously achieved.

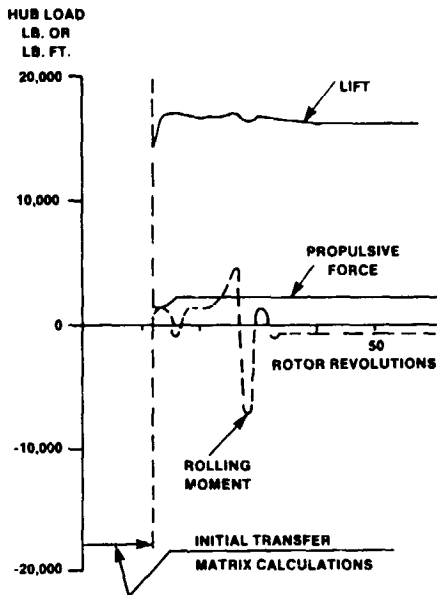


Fig. 5 Effects of Minimum Variance Controller on Steady Hub Loads For A Conventional Rotor

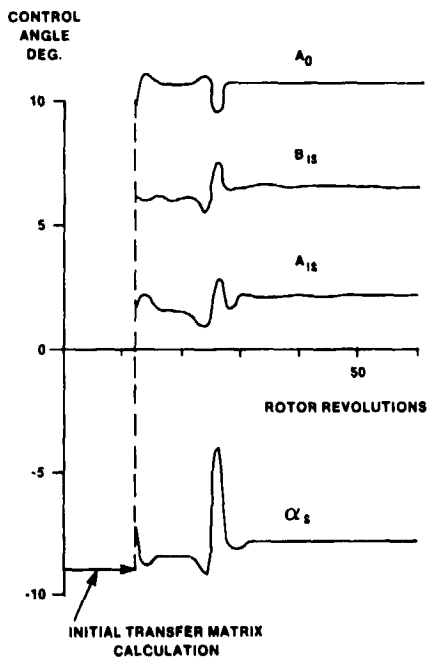


Fig. 6 Effects of Minimum Variance Controller on Trim Control Variables For A Conventional Rotor

The same approach lends itself to vibration reduction, with the vector of controlled variables containing coefficients of vibratory loads or accelerations at the blade passage frequency or at multiples of this frequency. Figures 7 and 8 show the effects of blowing controls on vibratory hub loads for a circulation control rotor, and the corresponding control state for selected blowing harmonics. A single blade analysis was used for this application although RDYNE is not limited to a single blade and can be used to reduce elastic airframe vibrations for a multi-blade rotor system.

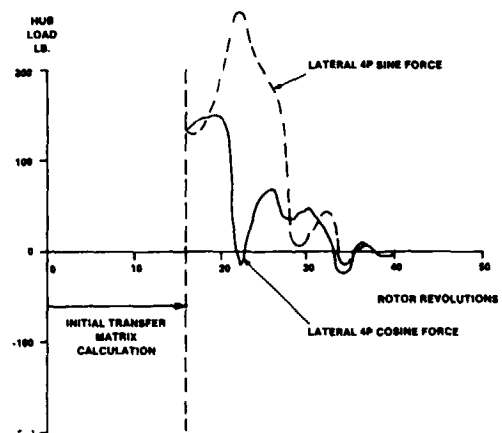
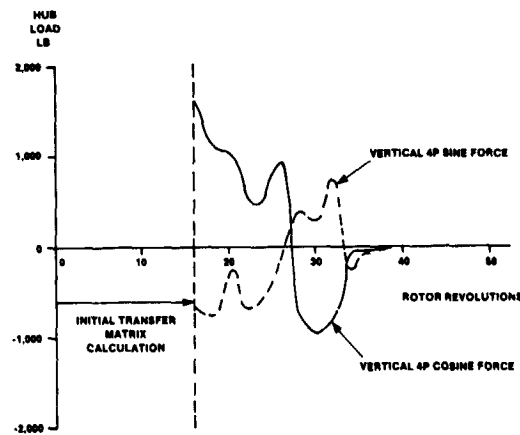


Fig. 7 Effects of Minimum Variance Controller on 4 Per Rev Hub Loads For Circulation Control Rotor



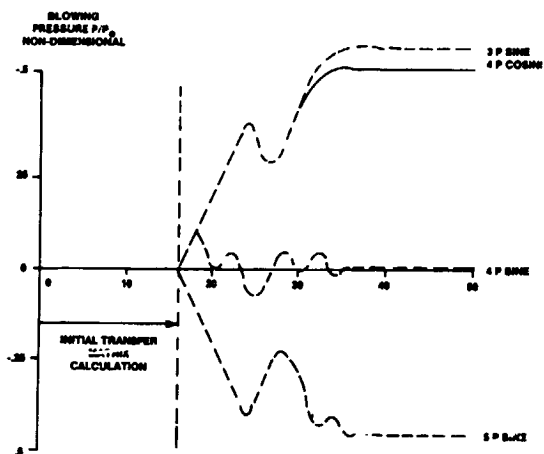


Fig. 8 Effects of Minimum Variance Controller on Control Variables For Circulation Control Rotor

The analysis is configured to permit selection of rotor load or vibration objectives, singly or in different combinations, and Figs. 9 and 10 show the combined effects of application of mechanical controls to achieve trim and vibratory hub load reduction.

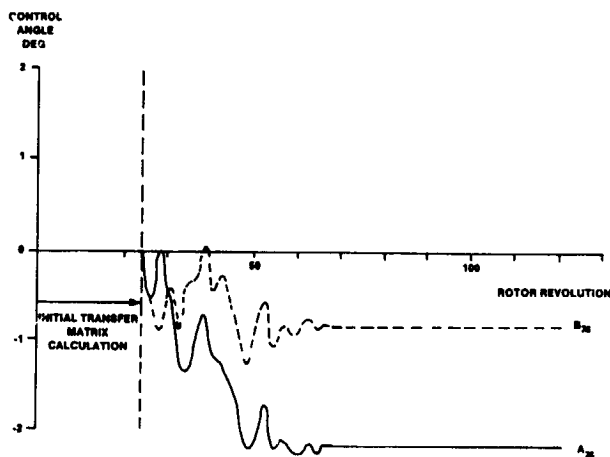
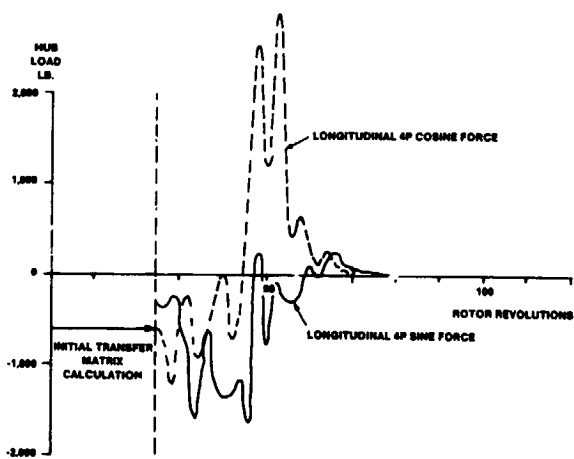
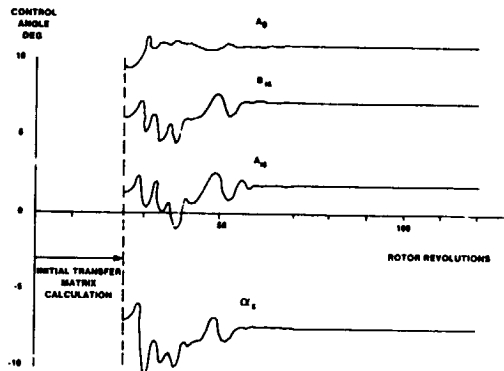


Fig. 10 Control Input History for Simultaneous Trim and Vibration Reduction on a Conventional Rotor

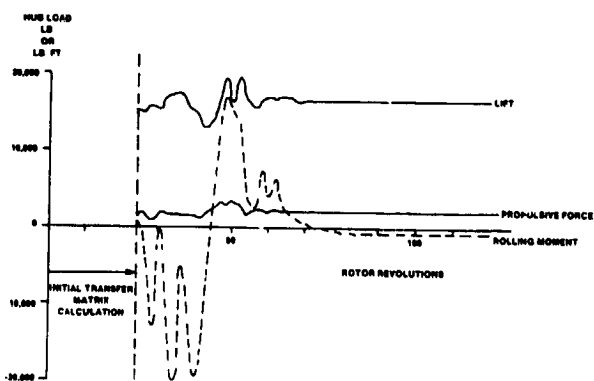


Fig. 9 Simultaneous Trim and Vibration Reduction on a Conventional Rotor

It is seen that a comprehensive solution such as the use of a single minimum variance controller for trim and vibration reduction can be used to reduce development costs by addressing more than one type of problem.

### Applications

Applications are described which show the comprehensive ability of RDYNE to handle stability and steady state vibratory load problems using a small number of elements and a time-history basis. Applications to new technologies are described.

### Ground Resonance Stability

In early 1979 RDYNE was evaluated for its ability to predict ground resonance stability involving the coupling of several articulated blades of the type shown in Table 1 to an elastic airframe. The elastic airframe was represented by a modal component (Table 1). The values of damping of the coupled systems were calculated from the decay in the responses of modal displacements in the airframe. FFT processing was not used. Figure 11 compares the percentage damping predicted by RDYNE with results from a linear stability analysis (Ref. 11) and shows very satisfactory agreement. Figure 12 compares stability boundaries from RDYNE with a Floquet solution (Ref. 12) for a rotor with a failed lag damper and again shows good agreement. The analysis is now used in a routine manner at Sikorsky to determine the stability of systems with failed lag dampers. It is seen that the time-history method can comprehensively treat problems which were solved by eigensolution and Floquet methods.

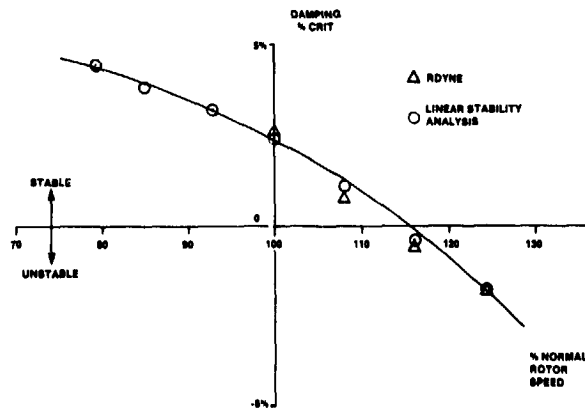


Fig. 11 Ground Resonance Stability Comparison Between RDYNE and Linear Stability Analysis

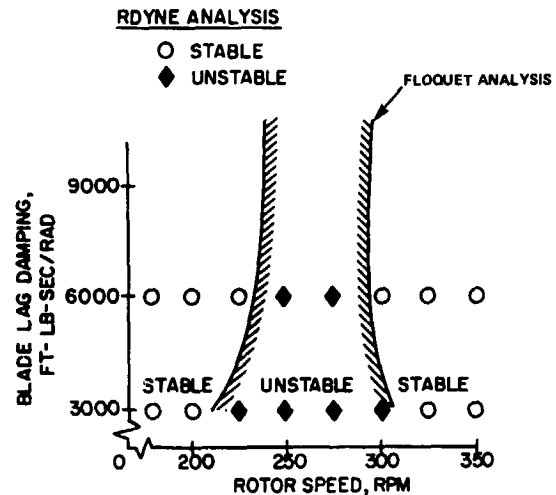


Fig. 12 Stability Boundaries Predicted by RDYNE and a Floquet Analysis for a Rotor with a Failed Lag Damper

### Non-symmetric Rotor and Damage Simulation

The advent of RDYNE created new opportunities for studying non-symmetric rotor and failure/damage simulations.

The program was applied to a BLACK HAWK rotor to simulate the response of a rotor/drive train system to lightning induced damage to one of the blades. The effects of lightning were determined by passing electric currents through a portion of blade in ground tests. The aerodynamic characteristics of the blade after damage were estimated from its appearance and were loaded in as input to the simplified section aerodynamic model listed in Table 2. The normal modes of the drive train were inserted in the input to the modal component to represent the seven component drive train. Results from the program without blade damage were used as initial conditions for a restart solution with the damaged blade. Figures 13 and 14 show blade and drive train responses before and after the damage. A drive train schematic is also shown in Figure 14. The transition from four-per-rev to once-per-rev responses is evident.

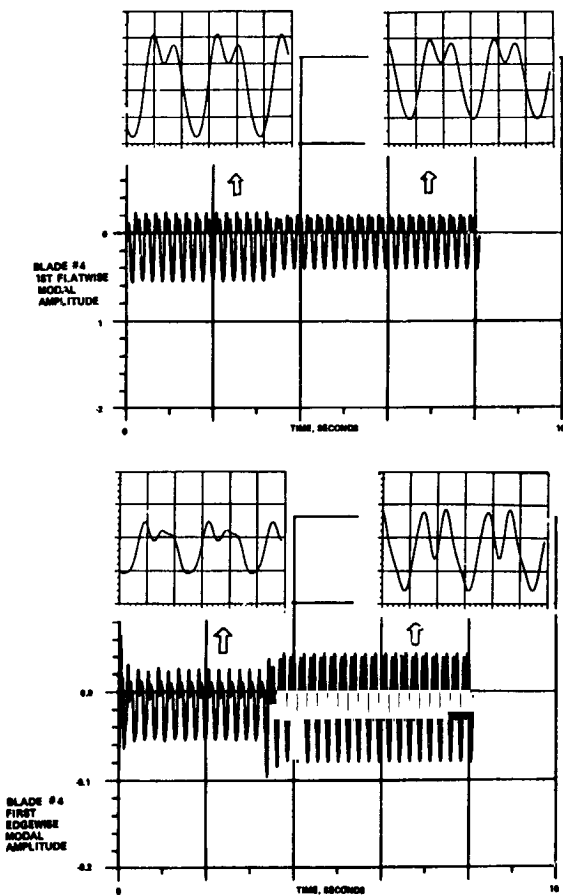


Fig. 13 Effects of Blade Damage on Time Histories of Blade Responses For A Coupled Rotor/Drive Train System

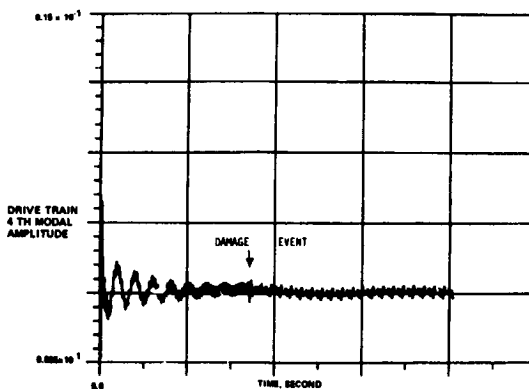
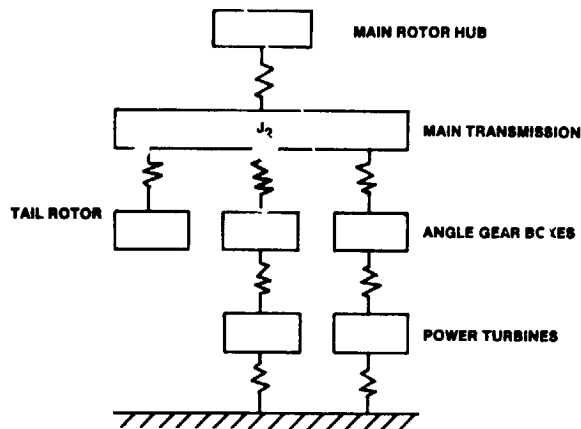


Fig. 14 Drive Train Responses to Rotor Damage For A Coupled Rotor/Drive Train System

The use of the modal component for the drive train in this problem and its use as an airframe in the ground resonance problems shows that versatility and reduced development cost can be achieved through using a single type of component for different types of problems.

#### Stopped and Gimballed Rotors

Stopped and gimballed rotors are new technologies to which RDYNE has been applied and for which it has provided timely solutions.

Rotors which are stopped have no centrifugal stiffening and have to be checked for bending divergence when in the swept-forward position. Figure 15 shows the increase with forward speed in damping of

the first elastic flatwise mode of a hingeless rotor blade stopped at 135 degrees azimuth. At the divergence speed the frequency of the mode is zero and the modal damping becomes infinite. The divergence speed agreed well with results predicted by the doublet lattice theory in the NASTRAN analysis. The ability of RDYNE to successfully model fixed lifting surfaces by means of an elastic blade component, originally derived for rotary wing applications, is the result of designing this blade component for multiple applications. In contrast to the original derivation in Ref. 8, which non-dimensionalized variables by rotor speed, the new equations were left in dimensional form, allowing the non-rotating case to be treated without difficulty.

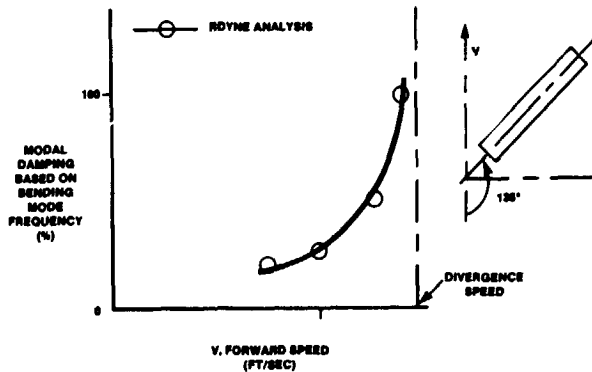


Fig. 15 Divergence of a 45 Degree Forward-Swept Stopped Rotor Blade

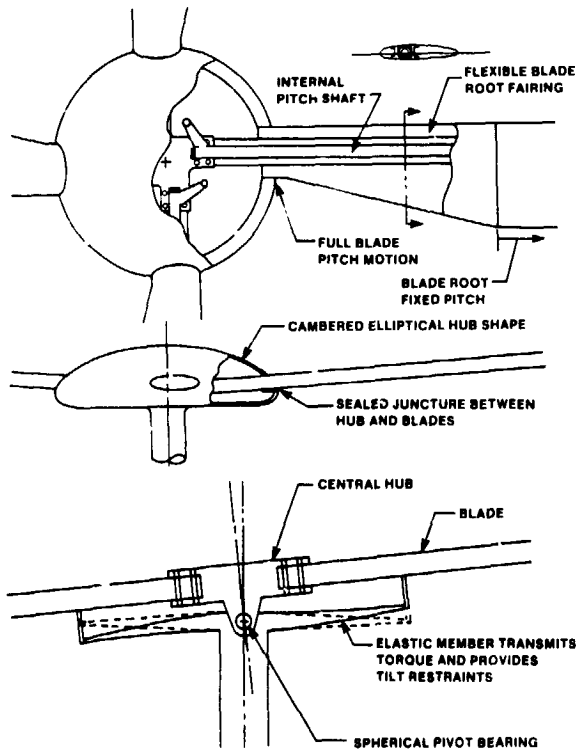


Fig. 16 General Arrangement of Dynaflex Rotor Hub and Schematic of Elastic Gimbal

The Dynaflex gimballed rotor is a new concept under development at Sikorsky which incorporates unique features (Ref. 13). Utilizing composite materials, the central hub is gimbal-mounted relative to the shaft achieving a universal joint action with a spring restraint to the tilting motion (Fig. 16). The arrangement is less cumbersome than a mechanical universal joint, and greatly reduces

Coriolis forces. Lower blade loads and reduced vibrations should result. The hub design is an exceptionally clean aerodynamic form.

Tests have been conducted with a 4.4 ft radius model. Comparisons shown below are for a stiff inplane rotor tested in a hover rig from 350 to 650 rpm, and for a soft inplane rotor tested at advance ratios between .15 and .45, and  $C_t/\sigma$  between .06 and .11.

RDYNE was applied to this rotor to evaluate its stability and vibratory load behavior. The analysis was modified in a period of two weeks to include the matrix substructure listed in Table 1 to simulate the gimbal. The short development was evidence of the responsiveness of a component-by-component method to new technology.

The rotor/support system used in model tests was represented by means of four elastic blades, a matrix substructure with two connection nodes representing the gimbal, and a normal mode structure representing the support (Fig. 17). The upper connection node of the matrix substructure was attached to the elastic blades, and the lower connection at the pivot bearing was attached to the normal mode support. The properties input to the matrix substructure were established by deriving gimbal mass, damping, and stiffness elements by the Lagrangian method. Stability results were obtained by means of a moving block method, and a single blade simulation was used to calculate the trim state of the gimbal rotor in level flight.

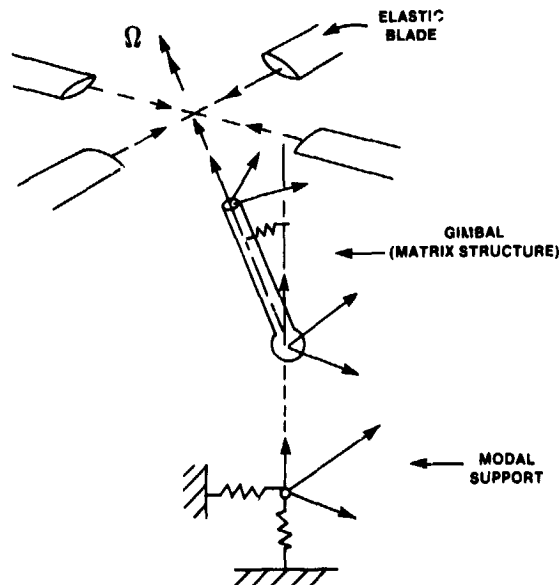


Fig. 17 Substructures Used to Represent the Dynaflex Rotor

Figure 18 compares test and analysis predictions of gimbal system frequencies and dampings in hover. Figure 19 compares test and analysis results for bending moments in level flight. Edgewise mode dampings established from a gauge on the moving blade are compared in Fig. 20. The hover stability comparisons are quite good as are flatwise bending moment variations with forward speed. The edgewise bending moments and stability in forward flight are overpredicted.

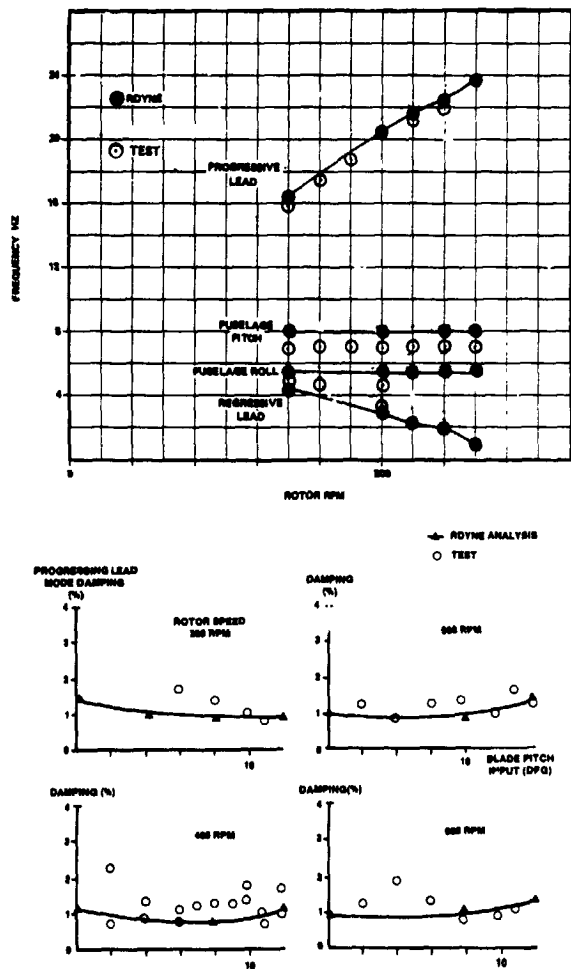


Fig. 18 Comparison of Predicted Frequencies and Dampings with Test Data For a Dynaflex Model Rotor in Hover.

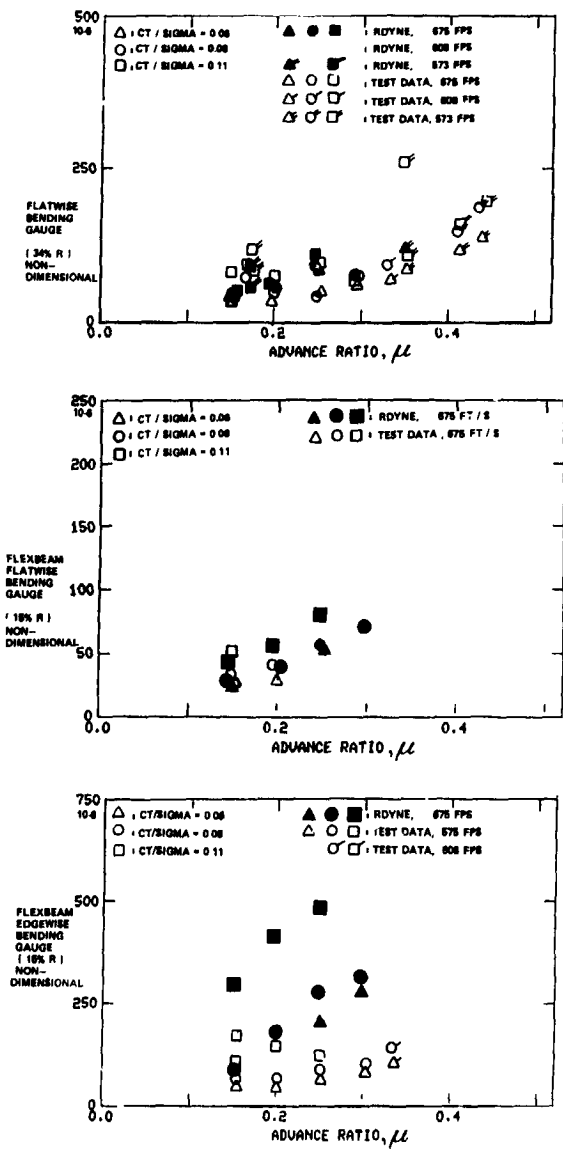


Fig. 19 Comparison of Vibratory Bending Moments for a Dynaflex Model Rotor in Level Flight.

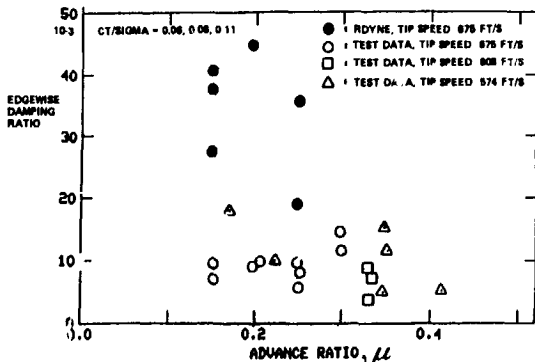


Fig. 20 Comparison of Blade Edgewise Stability for a Dynaflex Model Rotor in Level Flight.

#### Concluding Remarks

An analysis utilizing dynamical substructures and non-structural components has confirmed several desirable attributes expected from modern codes. These attributes include the ability to handle a comprehensive set of problems with a small library of components, supported by the ability to treat steady state vibratory and stability problems within a time-history framework. The analysis has responded to new technologies with timely solutions for advanced rotor concepts, by limiting the effort required to implement capabilities through its component structure. Comprehensive solutions, such as the use of a single minimum variance controller for trim and vibration reduction, have reduced development costs by addressing more than one type of problem.

#### References

1. Stevens, W.P., Myers, G.J., and Constantine, L.L., "Structured Design," IBM Systems Journal, Vol. 13, No. 2, 1974, pp. 115-139.
2. Sopher, R., Studwell, R.E., Cassarino, S., and Kottapalli, S.B.R., "Substructure Program for Analysis of Helicopter Vibrations," Journal of the American Helicopter Society, Vol. 28, No. 4, 1983, pp. 14-21.
3. Yen, J.G. and McLarty, T.T., "Analysis of Rotor - Fuselage Coupling and Its Effect on Rotorcraft Stability and Response," Vertica, Vol. 3, 1979, pp. 205-219.
4. Berman, A., "A Generalized Coupling Technique for the Dynamic Analysis of Structural Systems," Journal of the American Helicopter Society, Vol. 25, No. 3, July 1980, pp. 22-28.
5. Hurty, W.C., "Dynamic Analysis of Structural Systems Using Component Modes," AIAA Journal, Vol. 3, No. 4, 1965, pp. 678-685.
6. Chan, S.P., Cox, H.J., and Benfield, W.A., "Transient Analysis of Forced Vibrations of Complex Structural - Mechanical Systems," Journal of the Royal Aeronautical Society, Vol. 66, July 1962, pp. 457-460.
7. Chopra, I. and Johnson, W., "Flap-Lag-Torsion Stability of Circulation - Controlled Rotors in Hover," American Helicopter Society 34th Annual National Forum, May 1978.
8. Arcidiacono, P.J., "Prediction of Rotor Instability at High Forward Speeds - Volume 1 - Steady Differential Equations of Motion for a Flexible Helicopter Blade with Chordwise Mass Unbalance," USAAVLABS TR 68-18A, February 1969.
9. Landgrebe, A.J., and Egolf, T.A., "Rotorcraft Wake Analysis for Prediction of Induced Velocities," USAAMRDL TR 75-45, 1976.
10. Davis, M.W., "Development and Evaluation of a Generic Active Helicopter Vibration Controller," American Helicopter Society 40th Annual National Forum, Arlington, Virginia, May 1984.
11. Johnston, R.A. and Cassarino, S., "Helicopter Rotor Stability Analysis," USAAMRDL-TR-75-40, 1976.
12. Hammond, E.C., "An Application of Floquet Theory to Prediction of Mechanical Instability," Proceedings of the AHS/NASA Ames Specialists' Meeting on Rotorcraft Dynamics, NASA SP-352, Feb. 1974.
13. Fradenburgh, E.A. and Carlson, R.G., "The Sikorsky Dynaflex Rotor - An Advanced Main Rotor System for the 1990's," American Helicopter Society 40th Annual National Forum, Arlington, Virginia, May 1984.

DISCUSSION  
Paper No. 11

DEVELOPMENT AND APPLICATION OF A TIME-HISTORY ANALYSIS FOR ROTORCRAFT DYNAMICS  
BASED ON A COMPONENT APPROACH

Robert Sopher  
and  
Daniel W. Hallock

Marty Schroeder, Solar Energy Institute: You have talked about the modularity of your code and the flexibility of it--can you give some indication of the size of the code--RAM and ROM?

Sopher: It's actually 4 megabytes now. We are upgrading the IBM System to 8 megabytes so we are not that concerned about the size. We are not interested in overlay. At some point in time we may be interested in an executive which brings in only the routines that a user is interested in applying which would compile and link-edit the routines in object time to create a module which he was interested in using. So that's something we are interested in.

Ed Austin, U.S. Army Applied Technology Laboratory: I have just reams of questions I would like to ask. I'll try to cut it down to just a few. First, with regard to the aerodynamics. Have you given any consideration to the way your executive might handle aerodynamics that are not just a function of the current state but are dependent on previous events, maybe values of the state vector or other dependent parameters?

Sopher: We have given some consideration to that. For example, if you take the case of a general response in two-dimensional linear flow to an arbitrary impulse angle of attack change the response is provided by the Wagner function. In order to calculate the resulting lift you need to retain a history of what has happened to the motion and then you apply the kernel function to that. It's a very simple thing, actually. So as far as I can see in that particular application all you have to do is store the history of the motion somewhere in the program. In regard to other types of application I haven't really thought about anything other than that. Are you concerned about, say, a time-history representation of variable inflow?

Austin: Something like that, yes.

Sopher: [I have] not really thought about that very much.

Austin: Another question regarding your algorithms for your controller. You showed all your variables as nice continuous functions of time. Do you actually treat them that way or do you only look at them once per revolution?

Sopher: No. They go like this. They are discontinuous so really what I should have drawn was a set of . . . it would look something like a bar chart, but I just drew a smooth curve through that.

Austin: But what kind of algorithm is it that actually performs your convergence?

Sopher: Well, the objective function is a weighted square of the things you want to minimize. For example, say, you want to achieve a certain level of lift. It is the square of the difference between the target value of the lift and the actual lift as harmonically analyzed in the program, say, a steady value of lift. Now that is weighted by a weighting function. In addition to that we have weights that are applied to the control vector as well and the purpose of that is to try to limit the magnitude of the excursions of the controls because this is an unconstrained minimum optimization approach. We haven't tried to use a constraint optimization approach because if you go to any of those programs like COPES/COMMIN or ADS it's an incredibly large code and itself would equal the size of this program. So that's was the simple approach [that was] adopted. The relationship between the change in the state of the variables which are being used to control the system and the controlled state is obtained through what we call the T-matrix. That's identified subsequently by a Kaman filter method. As a matter of fact, I should make some acknowledgements here. Originally the controller was developed by John Molusis; Bob Taylor, who is with Boeing Vertol, went into further developments on it; and then our research labs carried out further developments. We had to reconfigure it considerably before it could be usefully used in RDYNE.

Austin: How often is that controller updated?

Sopher: Well, as often as you like. The user has the ability to define how often he wants to do it, but I believe in applications that we have typically it's after each revolution or after 2 revs or something like that. There are people who use the program who are more experienced in answering that question. It's undergoing fairly intensive use now.

Austin: You show some Floquet results. Do you use the one-pass or the N-pass approach?

Sopher: No, those results were obtained by means of a time-history response. But I compared with Gene Hammond's Floquet solution. We just use log decrement on that. In order to get the stability of the Dynaflex System we used a moving block method. As a matter of fact we haven't built the moving block into the program. Bob Goodman developed his own little post-processor. I think what would happen is you can eliminate some of the concerns about responsiveness in terms of time for providing stability results by building a post-processor into the program. That would address some of the concerns people have about the comparative efficiencies of aero-elastic stability methods versus time-history methods.

Austin: One final question. Do you have your aerodynamics and dynamics integrated into one program or they separate programs coupled by JCL?

Sopher: They are integrated into one program.